

STUDY ON CUTTING METHOD OF SAMPLING LUNAR SUPERFICIAL SOIL

by

**Kun-Chen HE^a, Ming-Zhong GAO^{a,b*}, Jing XIE^a,
Lei YANG^a, and Hai-Chun HAO^b**

^a State Key Laboratory of Intelligent Construction and Healthy Operation and Maintenance of Deep Underground Engineering, College of Water Resource and Hydropower, Sichuan University, Chengdu, Sichuan, China

^b State Key Laboratory of Intelligent Construction and Healthy Operation and Maintenance of Deep Underground Engineering, College of Civil and Transportation Engineering, Shenzhen University, Shenzhen, Guangdong, China

Original scientific paper

<https://doi.org/10.2298/TSCI2502209H>

Obtaining in-situ lunar soil samples is fundamental to studying the characteristics of lunar surface resources. A circular cutting sampling method is proposed, and its sampling characteristics are explored by theoretical analysis and numerical simulation. The results indicate that the traditional vertical cutting sampling will cause serious damage to the sequence structure and physical properties of samples. Circular inner blade cutting sampling can avoid the disorder of particle sequence, but the design of the inner blade will force the particles to move to the coring barrel, causing sample disturbance. Compared with vertical and inner-blade cutting method, circular outer blade cutting sampling reduces sample disturbance by 61% and 47.5%, respectively, making it the optimal sampling method. These research findings can provide theoretical and technical support for superficial sampling in deep space.

Key words: *in-situ sampling, resource exploration, lunar soil, circular cutting*

Introduction

The lunar surface is the most directly exposed object to space [1], and under the long-term bombardment of cosmic rays and micrometeorites, the lunar surface has formed a layer of finely fragmented deposits, lunar superficial soil [2, 3], which contains rich mineral, water ice, volatile resources [4, 5], providing crucial support for sustainable human development. In addition, the particle composition and sedimentary structure characteristics of lunar soil also record the evolutionary history of lunar materials and the processes of space weathering [6-8], making it significant to obtain in-situ samples of lunar soil. Currently, lunar sampling is the only way to obtain lunar superficial soil. Since the 20th century, the former Soviet Union, the USA, and China have successively conducted lunar sampling missions and returned samples to Earth [9-11]. These countries' sampling devices can be categorized into penetrative and non-penetrative sampling methods based on their approach. Non-penetrative sampling methods include shoveling, gripping, raking, and excavation. Due to the significant destruction caused by these methods, the structural characteristics of the samples obtained have been completely destroyed [12]. Penetrative sampling is currently the mainstream method, which can be further divided

* Corresponding author; e-mail: 13808018702@163.com

into dynamic drilling and static pressing based on sampling depth [13, 14]. Static pressing is the primary method for shallow sampling, using a thin-walled cylindrical corer to vertically penetrate lunar soil. However, during the sampling process, the sample is subjected to frictional forces from the cylinder boundary, resulting in dislocation of the sequence structure of the sample. Additionally, due to the minimal cohesion between particles, it makes it challenging to successfully extract lunar soil.

In conclusion, the in-situ information carried by lunar soil is of significant importance for interpreting the characteristics of lunar resource and lunar evolution history. However, there are still technical issues with undisturbed sampling in the lunar superficial soil [15-17]. This paper proposes a circular cutting sampling method, elaborating on its mechanical design key points. It compares the destructive characteristics of vertical and circular cutting sampling through theoretical derivation and discrete element simulation and demonstrates the superiority of the circular cutting sampling method.

Scheme introduction

Introduction of circular cutting scheme

The circular cutting sampler consists of three parts: Dowel steel, extension handle and Coring institution, fig. 1. The Coring institution is composed of six parts, including retaining plate, breaker, outer cylinder and inner core. When sampling, press down Coring institution through extension handle and then rotate inner core for circular cutting sampling. The breaker is designed as a semi-cone with a diameter of 4 cm and an angle of 30° , which can ensure that the lunar soil on the coring surface is not disturbed during the penetration of the coring device.

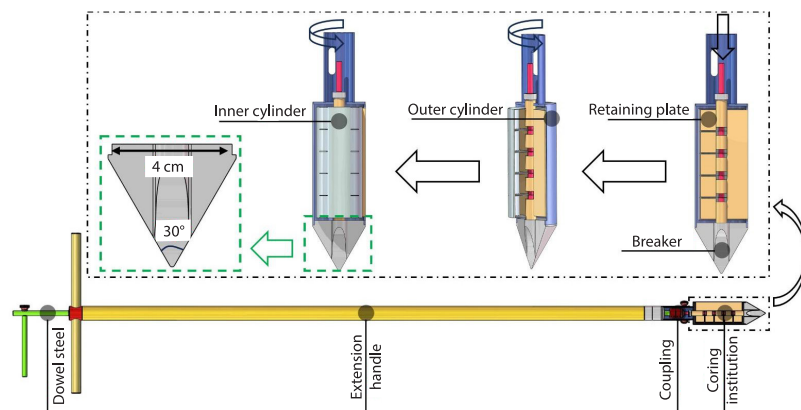


Figure 1. Circular cutting scheme design

Experimental scheme

Discrete element method is used to simulate the vertical and circular cutting sampling process. In order to reflect the sedimentary sequence of the lunar soil [18], establishing layers of coarse particles with a diameter of 0.15 mm and fine particles with a diameter of 0.15 mm. Ultimately, lunar soil simulant with the density of $1431\sim 1558.2\text{ kg/m}^3$ was obtained, which closely approximates the true density of lunar soil obtained by Olhoeft GR ($1500 \pm 50\text{ kg/m}^3$) [19]. Therefore, this model can reflect the mechanical properties of lunar soil. Additionally, to conserve computational resources, the radius of the corer was reduced to 5 mm with a penetration depth of 3 mm. other computational parameters are detailed in tab. 1.

Table 1. Model calculation parameters

Grain density	2300 kg/m ³	Particle's elastic modulus	10.5 GPa	Particle poisson's ratio	0.25
Corer density	4.5 kg/m ³	Corer's elastic modulus	118.6 GPa	Corer poisson's ratio	0.33
Gravity	1.618 m/s ²	Penetration speed	0.75 mm per second	Penetration depth	3 mm
Angular speed	45° per second	Corer diameter	8 mm	Domain diameter	10 mm

Result discussion

Vertical cutting sampling feature

Vertical cutting sampling (VCS) was simulated according to the parameters in tab. 1, and the results are shown in fig. 2. From the figure, it can be observed that as the corer performed vertical cutting, particles inside the core tube were disturbed. The particles near the cylinder wall are affected by the friction force, F_f , and move vertically downward linearly. This resulted in fine particles embedding into the coarse particle layer, with displacement decreasing gradually away from the inner wall. Because the coring blades is right triangular configuration with the hypotenuse facing outward, outer particles undergo parabolic motion under the pressures of blade edge pressure, F_p , and F_f during the VCS. Additionally, as vertical cutting progresses, the average velocity of inner particles fluctuates and rises, fig. 2(b), particularly when the corer enters the coarse particle layer. This shows that the deeper the vertical cutting, the more severe the disturbance of the sample. According to the calculation results, the total average speed of the sample particles during the VCS is 0.108 mm per second. During the cutting process, the density of particles inside the cylinder increased from 1415.35-1492.12 kg/m³, with an increase of 5.4%. Thus, under the effect of vertical cutting, the upper fine particles will be embedded in the lower coarse-grained layer, the particle structure sequence will be seriously destroyed, and the physical parameters of the sample will also change greatly.

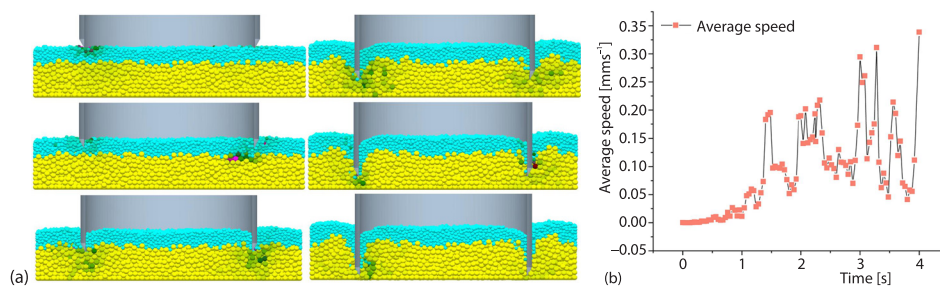


Figure 2. Simulation results of vertical cutting;
(a) process of VCS and (b) average particle velocity

Circular cutting sampling feature

In order to avoid the disorder of particle sequence in sampling [20], the circular cutting coring is proposed. According to the different blade configurations, two types of blades are designed: inner blade and outer blade, fig. 3.

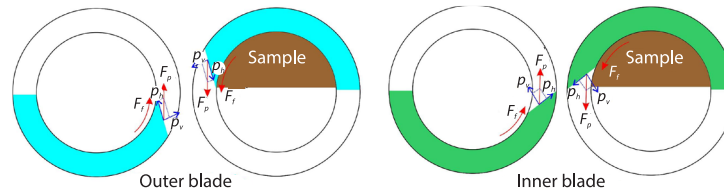


Figure 3. Circular cutting blade structure

Circular inner blade cutting method

Simulated the circular inner blade cutting sampling (CICS) according to tab. 1, with results shown in fig. 4. From the trajectory diagram of sampling particles, fig. 4(a), it can be observed that during the cutting process, the particle motion can be mainly classified into two types. The first type is a circular motion trajectory formed by particles under the action of F_f . This motion causes interlayer particle displacement, but due to the small F_f , its influence is limited. The second type is a complex trajectory formed by the pressure, F_p , squeezing the particles at the blade. Similarly, this trajectory only causes intralayer particle displacement. However, due to stress concentration at the blade, it causes the most extensive disturbance to sample particles. According to the stress decomposition diagram of the CICS in fig. 3, F_p is parallel to the tangential direction of the blade, with component, p_v , perpendicular to the blade surface and directed towards the inner side of the corer. This causes the particles in front of the blade to be squeezed toward the inner side of the corer, fig. 4(a), and the particle trajectory mainly forms an inward arc. Furthermore, due to squeezing, samples experience a certain degree of *heightening* after sampling is completed. In addition, the calculation results show that the total average velocity of sample particles is 0.08 mm per second, fig. 4(b). In the process of CICS, the average particle velocity varies significantly over time without a clear trend. The particle density also increased from 1558.02-1633.75 kg/m³, a rise of 4.8%. In conclusion, under the CICS, the particle motion trajectory is horizontal, particle stratigraphy is preserved, but due to the squeeze of component p_v , the sample particles are disturbed.

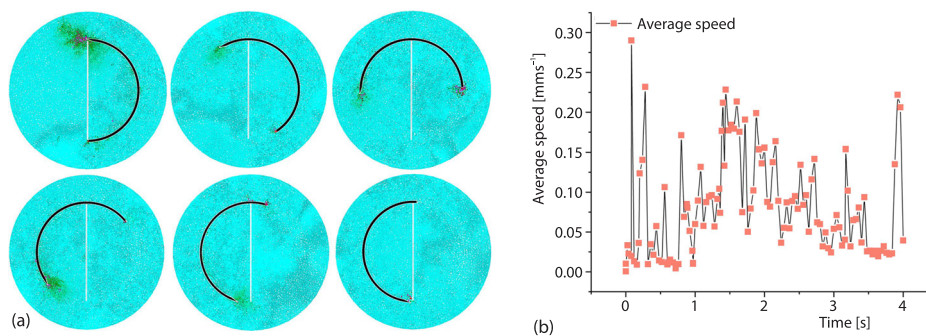


Figure 4. Calculation results of CICS; (a) process of CICS and (b) average particle velocity

Circular outer blade cutting method

Keeping the angular speed constant, the simulation result of circular outer blade cutting sampling (COCS) is shown in fig. 5. The figure shows that the trajectory of particles is similar to that of CICS, with the only difference being that in the process of COCS, the com-

ponent p_v of pressure, F_p , to point outward of the coring barrel. Therefore, under the squeezing action of the blade, particles primarily move towards the outer side of the coring barrel, fig. 5(a), resulting in the increase of the particle height outside the coring barrel. In contrast, the sample inside the coring barrel is less squeezed and disturbed. Figure 5(b) shows that the total average speed of particles under process of COCS is 0.042 mm per second, with smaller fluctuations in particle average velocity compared to that of CICS. The density varies from 1431.9-1462.7 kg/m³, with an increase of 2.1% post-cutting. Therefore, under COCS, the structural characteristics of particles can be well preserved.

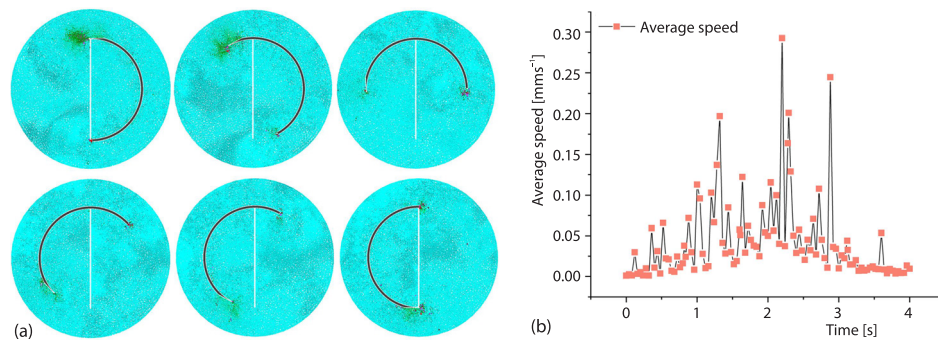


Figure 5. Calculation results of COCS; (a) process of COCS and (b) average particle velocity

Comparison of cutting methods

Taking particle density and average speed as disturbance indexes, comparing with three coring schemes, VCS, CICS, and COCS, it can be seen that the VCS has the greatest damage to the sample, with the total average velocity of particles being 0.108 mm per second and the density increasing by 5.4%. However, the COCS has the least damage to the sample, and the total average particle velocity is 0.042 mm per second, and the density increases by 2.1%. Compared with the CICS and the VCS, we find that the particle disturbance degree decreases by 47.5% and 61%, and the fidelity of physical parameters increases by 229% and 257%, respectively. Therefore, in the sampling task of shallow lunar soil, the COCS can better preserve the structural and physical parameter characteristics of the sample, making it the optimal sampling method.

Conclusion

Based on the theoretical analysis and numerical simulation, we get the following conclusion. In the vertical cutting mode, the trajectory of sample particles is linear and parabolic, and the sequence of sample particles is destroyed. The total average speed of particles reaches 0.108 mm per second, and the density increases by 5.4%, which is the most destructive to the sample. The circular inner blade cutting method can preserve the particle sequence of the sample well. The total average speed of particles is 0.08 mm per second, and the density increases by 4.8%. The sample experiences a *heightening* phenomenon, which is destructive to the sample. The circular outer blade cutting method is the optimal method for lunar superficial soil sampling tasks, with the pressure component, p_v , directed towards outside of the coring barrel, resulting in minimal impact on the sample. Compared to vertical cutting and circular inner blade cutting methods, particle disturbance is reduced by 61% and 47.5%, respectively.

Acknowledgment

This work was financially supported by the National Key Research and Development Program of China (2023YFF0615404) and National Natural Science Foundation of China (52225403, U2013603).

Nomenclature

F_f – frictional force, [N]
 p_v – vertical component of F_p , [N]

F_p – pressures of blade edge pressure, [N]
 p_h – horizontal component of F_p , [N]

References

- [1] Lucey, P., et al., Understanding the Lunar Surface and Space-Moon Interactions, *Reviews in Mineralogy and Geochemistry*, 60 (2006), 1, pp. 83-219
- [2] Johnson, J. R., et al., Spectrogoniometry and Modelling of Martian and Lunar Analog Samples and Apollo Soils, *Icarus*, 223 (2013), 1, pp. 383-406
- [3] Li, J. H., et al., Rapid Screening of Zr-Containing Particles from Chang'e-5 Lunar Soil Samples for Isotope Geochronology: Technical Roadmap for Future Study, *Geoscience Frontiers*, 13 (2022), 3, ID101367
- [4] Chen, Z. H., et al., The Contact Force Between Lunar-Based Equipment and Lunar Soil, *iScience*, 27 (2024), 4, ID109322
- [5] Zhang, X., et al., Presence of Non-Solar Derived Krypton and Xenon-Unveiled by Chang'e-5 Lunar Soils, *Earth and Planetary Science Letters*, 637 (2024), 7, ID118725
- [6] Liu, T., et al., Research on the Retention Characteristics of the Stratification Information of Lunar Soil Drilling Sampling, *Advances in Space Research*, 66 (2020), 10, pp. 2428-2445
- [7] Liu, T., et al., Effect of Drill Bit Structure on Sample Collecting of Lunar Soil Drilling, *Advances in Space Research*, 68 (2021), 1, pp. 134-152
- [8] Zhao, G., et al., Investigation on the Disturbance of the Bedding Information of Lunar Soil Samples in Flexible Tube Coring Missions, *Acta Astronautica*, 170 (2020), 5, pp. 37-45
- [9] Gawronska, A. J., et al., New Interpretations of Lunar Mare Basalt Flow Emplacement from XCT Analysis of Apollo Samples, *Icarus*, 388 (2022), 12, ID115216
- [10] Marov, M. Y., et al., Early Steps Toward the Lunar Base Deployment: Some Prospects, *Acta Astronautica*, 181 (2021), 4, pp. 28-39
- [11] Toklu, Y. C., et al., Production of a Set of Lunar Regolith Simulants Based on Apollo and Chinese Samples, *Advances in Space Research*, 72 (2023), 2, pp. 565-576
- [12] Zhang, X., et al., A Review of Sampling Exploration and Devices for Extraterrestrial Celestial Bodies, *Space Science Reviews*, 218 (2022), 8, ID59
- [13] Litvak, M., et al., Luna – 25 Robotic Arm: Results of Experiment with Analog of Lunar Regolith in Lunar Like Conditions, *Acta Astronautica*, 200 (2022), 11, pp. 282-290
- [14] Badescu, M., et al., Rotary Hammer Ultrasonic/Sonic Drill System, *Proceedings, IEEE International Conference on Robotics and Automation, IEEE, Pasadena, Cal., USA, 2008*, pp. 602-607
- [15] Gao, Y., et al., Planetary Micro-Penetrator Concept Study with Biomimetic Drill and Sampler Design, *IEEE Transactions on Aerospace and Electronic Systems*, 43 (2007), 3, pp. 875-885
- [16] Li, F., et al., Formation Mechanism of Core Discing During Drilling under Deep in-Situ Stress Environment: Numerical Simulation and Laboratory Testing, *Journal of Central South University*, 30 (2023), 10, pp. 3303-3321
- [17] Lin, Y., et al., Return to the Moon: New Perspectives on Lunar Exploration, *Science Bulletin*, 69 (2024), 13, pp. 2136-2148
- [18] Chen, Z., et al., Numerical Investigation on the Sieving Performance of Elliptical Vibrating Screen, *Processes*, 8 (2020), 9, ID1151
- [19] Carrier, W. D., et al., A User's Guide to the Moon, *Physical Properties of the Lunar Surface*, 72 (1991), 7, pp. 475-594
- [20] Wang, J., et al., Experimental and Analytical Studies on Behavior of Shape Memory Alloy-Based Knife-Edge Seal System for Extraterrestrial Soil Sample Return Mission, *Vacuum*, 222 (2024), 4, ID 113048